Journal of Experimental Nanoscience
Publication details, including instructions for authors and subscription information:
http://www.informaworld.com/smpp/title~content=t716100757

Investigating the cellular response to nanofibrous materials by use of a multi-walled carbon nanotube model

J. H. George[a]; M. S. Shaffer[b]; M. M. Stevens[ac]
[a] Department of Materials, Imperial College London, South Kensington, SW7 2AZ [b] Department of Chemistry, Imperial College London, South Kensington, SW7 2AZ [c] Institute for Biomedical Engineering, Imperial College London, South Kensington, SW7 2AZ

Online publication date: 28 September 2010

To cite this Article George, J. H. , Shaffer, M. S. and Stevens, M. M.(2006) 'Investigating the cellular response to nanofibrous materials by use of a multi-walled carbon nanotube model', Journal of Experimental Nanoscience, 1: 1, 1 — 12
To link to this Article: DOI: 10.1080/17458080500463149
URL: http://dx.doi.org/10.1080/17458080500463149

Journal of Experimental Nanoscience,
Vol. 1, No. 1, March 2006, 1–12

Taylor & Francis
Taylor & Francis Group

Investigating the cellular response to nanofibrous materials by use of a multi-walled carbon nanotube model

J. H. GEORGE†, M. S. SHAFFER‡ and M. M. STEVENS*†§

†Department of Materials, Imperial College London,
South Kensington, SW7 2AZ
‡Department of Chemistry, Imperial College London,
South Kensington, SW7 2AZ
§Institute for Biomedical Engineering, Imperial College London,
South Kensington, SW7 2AZ

(*Received October 2005; in final form November 2005*)

One motivation for synthesizing nanofibrous materials is the desire to mimic interactions between cells and the natural extracellular matrix. The cellular response to nanofibre assemblies of differing length-scales and densities of nanofibres is of direct interest; in this study, we investigate the response of human lung epithelial cells (A549), osteoblast-like cells (MG63), and primary osteoblast cells to a model nanofibre system over a seven-day period. A low-density array of multi-walled carbon nanotubes (MWCNTs) (dia. 35 nm) provides a non-degradable, stiff, nanofibrous surface for cell culture investigation. We find that cells attach and survive on MWCNTs, although proliferation is not as rapid as on flat control substrates. Immunofluorescent vinculin staining revealed that small point-contacts are produced by cells attached to MWCNTs. Larger focal adhesions, as typically found in two-dimensional surface culture, were not seen for cells attached to the nanotube substrates. The MWCNT arrays provide a simple, yet effective, model system with which to develop a better understanding of cell responses to nanofibrous constructs which are relevant to tissue engineering and regenerative medicine.

Keywords: Cell; Carbon nanotube; Nanotube; Nanofibre; Focal adhesion

1. Introduction

In this study, we investigate the response of attachment-dependent cells to multi-walled carbon nanotubes (MWCNTs). Carbon nanotubes (CNTs) have many unique properties that, in addition to their nanoscale-dimensions, set them apart from other nanofibrous materials for potential biological use. They are intrinsically stiff and strong, and can readily be incorporated in polymer composite materials, including those based on natural fibres such as collagen [1]. Their electrical properties have stimulated attempts to fabricate constructs for interface with the nervous system and

*Corresponding author. Email: m.stevens@imperial.ac.uk

Journal of Experimental Nanoscience
ISSN 1745-8080 print/ISSN 1745-8099 online © 2006 Taylor & Francis
http://www.tandf.co.uk/journals
DOI: 10.1080/17458080500463149

the repair of neural damage [2, 3]. Their superior mechanical properties have encouraged applications in bone scaffold materials [4, 5].

For *in vivo* applications, the long-term toxicity of CNTs remains to be established. Initial studies using both single-walled carbon nanotubes (SWCNTs) [6–9] and MWCNTs [10] indicate that oxidative stress and the formation of granulomas may cause tissue damage, as cells endeavour to engulf and breakdown individual nanotubes. Our motivation for investigating the cellular response to MWCNTs is not to build constructs for direct implantation, but to create model systems that facilitate the exploration of the cellular response to nanofibrous materials in general. By using chemical vapour deposition [11], large-scale production of uniform nanotubes with controlled diameters (10–300 nm), lengths (10 μm–5 mm) and densities can be achieved. The nanotubes are far stiffer and stronger than other nanofibres of similar dimensions, providing a fixed structure for cellular interaction. In cell culture, after adsorbing a protein coat, their dimensions and surface chemistry may be similar to many other nanofibrous systems currently under development, although their intrinsic stiffness is higher.

Interest in the development and use of nanofibrous materials for tissue engineering, drug delivery and wound healing [12–16] is increasing. A range of emerging technologies is being employed to fabricate nanofibrous constructs, including electrospinning (for bone [17], vascular [18] and neural tissue scaffolds [19]), phase separation [16], and self-assembly of synthetic amphiphiles [20, 21], peptides [22] and proteins [23, 24]. Nanofibres have similar dimensions to collagen and other major proteins of the extracellular matrix (ECM). At these dimensions, subcellular-sized porosity is increased, which can result in enhanced cellular invasion and increased diffusion of nutrients and cell signalling molecules throughout the scaffolds. Nanofibrous scaffolds also support a larger surface-to-volume ratio than conventional scaffolds, potentially allowing for the selective binding of cell recognized ligands at higher densities [25]. The fine scale of the chemical texture, in combination with the high porosity of fibrous materials, enables cells to grow isotropically, unless nanofibre orientation is deliberately introduced. Many challenges remain, especially the need to match the structural properties to tissues and applications, and the need to understand how differences in length-scale and surface chemistry relate to protein adsorption, cell attachment and response.

For attachment-dependant cells, adhesion to a base substrate is essential for cell survival; this interaction is highly dependent on the surface type, topology, and surface chemistry. On contact with a surface, specific ligand binding at the cell membrane leads to the formation of focal adhesions (FAs) [26] which initiate a process of surface interaction leading to intracellular signalling. FAs are multi-protein complexes which connect specific bound domains in extracellular proteins through the cell membrane (via integrins [27]) to cytoskeletal proteins supporting the cell. The underlying substrate directly affects the size, positioning and motility of FAs and thus the cellular response to the underlying substrate [28].

Our results show that although cells attach equally to both non-dense nanotube meshes and flat control surfaces, it is likely that the dimensions and spacing of nanotubes are important factors in determining subsequent cell spreading and proliferation.

2. Materials and methods

2.1. *Fabrication and characterization of MWCNT surfaces*

MWCNT arrays were fabricated by chemical vapour deposition [11]. Briefly, a solution of ferrocene (3 wt.%) in toluene was injected at 4 ml/hr into a furnace preheated to 760°C, with an atmosphere of argon and 10% hydrogen (with a flow rate of 500 ml/min). Over a period of 4 hr, MWCNTs were grown from square quartz substrates ($10 \times 10 \times 4$ mm) placed inside the furnace. A LEO 1525 Gemini Field Emission Scanning Electron Microscope (SEM) (with micro-X-ray analysis capability) was used to determine the size and composition of the nanotubes. X-ray counts were recorded over three separate areas (60×40 μm) during a five-minute period at 15 keV. ImageJ software (National Institute of Health, USA) was used to threshold the SEM images, observing that the uppermost nanotubes were most brightly illuminated. These images provide a visual approximation of the available surface area for cell attachment. Sterilization was achieved by immersing the surfaces in 100% ethanol for 1 hr, and then washing with PBS for 20 minutes per wash (3×). After initial submersion, the surfaces were kept wet, to prevent bunching of the nanotubes.

For a comparative control, surfaces of highly orientated polymorphic graphite (HOPG) (SPI supplies, USA) were cleaved from a 10×10 mm block and affixed to glass coverslips. Borosilicate glass coverslips (13 mm dia.) were used as a standard control. Both surfaces were autoclaved to sterilize before use in culture.

2.2. *Cell culture and surface seeding*

Three cell types were investigated: the human osteosarcoma cell line (MG63) (ECACC, UK), the human lung epithelial carcinoma cell line (A549) (ATCC, USA), and primary foetal osteoblasts at third passage (FOB, kind gift of Dr R. Bielby, Chelsea and Westminster Hospital). The MG63 cells were routinely cultured in 75 cm^2 flasks using Dulbecco's modified Eagles' medium (DMEM), the A549 cells using Ham's F12, and the FOB cells using DMEM-F12 (1 : 1) (all supplied by Gibco, UK). Each medium was supplemented with 10% foetal bovine serum (FBS) (Gibco, UK) and 1% antibiotic/antimycotic (Sigma, UK) (complete medium). Initial culture was performed in 75 cm^2 flasks at 37°C in a humidified atmosphere with 5% CO_2. At 70% confluence, cells were detached using trypsin-ethylenediaminetetraacetic acid (EDTA) (Sigma, UK), and cell count was determined by haemocytometer. Cells were resuspended to the appropriate concentration for seeding in complete medium. Previously, samples (represented in triplicate) had been placed into 24 well plates and preconditioned with complete medium for 1 hr at 37°C. Cells were seeded onto the samples at densities of 2×10^3 cells/cm^2 and incubated at 37°C, 5% CO_2. Culture media were replaced after each two-day period.

2.3. *Cell proliferation assay*

After one and seven days, the standard protocol for a commercially available colorimetric proliferation assay was used to quantify cell proliferation (CellTiter 96®

Aqueous One Solution Cell Proliferation Assay, Promega, UK). Briefly, samples were transferred to 24 well plates, and washed (1×) with phosphate buffered saline (PBS) (Invitrogen, UK). 600 µl of DMEM phenol free medium (Gibco, UK) supplemented with 120 µl One Solution Reagent was added to each well. The samples were incubated for 2 hr at 37°C, 5% CO_2, after which the medium above the samples was removed and transferred to 96 well plates for reading at 492 nm, using an Anthos 2020 microplate absorbance reader.

2.4. *Analysis of cell attachment, spreading and visualization of focal adhesions*

After 24 hr, samples were washed in PBS and fixed in paraformaldehyde (PFA) (Sigma, UK) (4% w/v in PBS) for 30 minutes. Cells were then permeabilized by use of a 0.5% Triton-X-100 permeabilizing buffer (TXB) for 25 minutes (10.3 g sucrose, 0.292 g NaCl, 0.06 g $MgCl_2$, 0.476 g Hepes Buffer, and 0.5 ml Triton-X-100 in 100 ml distilled water), then washed in immunofluorescence buffer (IFB), containing 0.1% Triton X-100 and 0.1% BSA in PBS [29]. The samples were incubated with commercially available monoclonal mouse anti-human vinculin antibody (Sigma) (2 µl/ml in IFB) for 1 hr, washed in IFB (3×), incubated with a biotinylated rabbit anti-mouse antibody (2 µl/ml in IFB) for 1 hr, washed in IFB (3×), and incubated with a streptavadin-TX Red developer (2 µl/ml in IFB) together with FITC conjugated phalloidin (2 µg/ml) (Sigma, UK) for 1 hr. Finally, samples were washed in IFB (3×) and mounted with VECTASHIELD® mounting medium containing 4′,6-Diamidino-2-phenylindole (DAPI) (Vector Labs, UK). To serve as a control, the primary antibody was omitted to test for secondary antibody specificity. To determine cellular response after seven days in culture, samples were washed in PBS, fixed in PFA for 30 minutes, permeabilized in TXB for 25 minutes and fluorescently stained (as above) with FITC conjugated phalloidin (2 µg/ml) for 1 hr, then washed in IFB (3×) and mounted with VECTASHIELD® mounting medium containing DAPI. An Olympus BX51 fluorescence microscope was used to image the samples. Attachment at one day was determined by counting cells in random fields of size 0.59 mm^2 ($n > 10$). ImageJ software was used to analyse cell spreading at one day, by using a process of image thresholding to identify cell boundaries and pixel counting to determine individual cell area ($n > 40$ cells).

2.5. *Visualization of cell attachment to MWCNTs by scanning electron microscopy*

After 24 hr, cells were fixed in 2.5% glutaraldehyde in PBS for 40 minutes at 4°C, then rinsed in PBS and dehydrated through a series of graded ethanol (25%, 50%, 75%, 90%, 2 × 100%) in distilled water at five-minute intervals. Finally the samples were critical point dried by incubating twice in hexamethyldisilazane (Sigma, UK) for five minutes and left to air-dry. The samples were imaged at low voltage (1.5 kV), using the LEO SEM mentioned above, to reveal cell morphology and surface interaction.

3. Results

3.1. *MWCNT surface morphology, hydrophobicity and EDX analysis*

We used SEM imaging to characterize the MWCNT surfaces, and found the average nanotube diameter to be 35 ± 10 nm (table 1). EDX analysis revealed that trace amounts of iron catalyst remained in the MWCNT samples after fabrication. Previously, we have found that the removal of this catalyst by an acid leaching process did not significantly alter the cellular attachment and spreading on the surfaces (data not shown). Nanotubes grew vertically on the quartz substrates, reaching 500 nm in length (figure 1A). CNTs are inherently hydrophobic (figure 1B); however, exposure to a surfactant such as 0.5% Triton X-100, or to serum proteins in culture media reverses the wetting behaviour [30]. The CNTs almost certainly become wettable in this way, through a shielding process, where the formation of a surfactant or protein coat presents hydrophilic groups at the surface of the nanotubes.

Table 1. MWCNT characterization through SEM image analysis and EDX analysis.

MWCNT properties			
Diameter	35 nm	±10 nm	($n = 30$)
Composition (atomic) (weight)	Carbon: 98.04 ± 0.03% Carbon: 91.48 ± 0.13%	Iron: 1.96 ± 0.03% Iron: 8.52 ± 0.13%	($n = 3$)

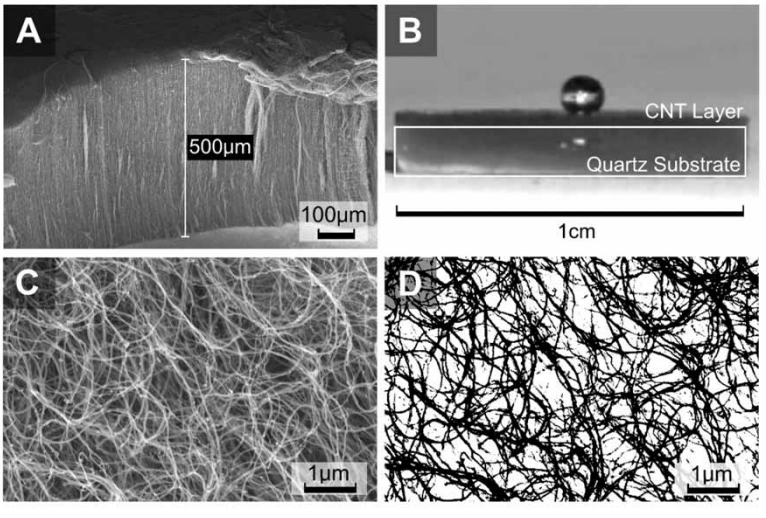

Figure 1. SEM imaging revealing a vertically aligned carpet-like layer of MWCNTs (A). From the water drop profile (B), it is evident that CNTs are extremely hydrophobic before encountering serum proteins in cell culture medium. The uppermost layer (C) is made up of a non-dense, randomly oriented network of nanotubes (EHT = 5 kV, WD = 8 mm, Mag = ×50 k). The sample area available for cell adhesions can be visualized by taking a threshold of the SEM image (D).

The SEM images revealed that, although the bulk of nanotube growth is aligned, the uppermost sample layer consists of a low-density network of randomly oriented nanotubes (figure 1C); previous studies have shown that initial growth is often misaligned. Visual analysis reveals that this layer of nanotubes provides a combined solid area that is substantially less than the total sample area (figures 1C, D). Assuming that the cells do not penetrate the network, the open structure provides less area for initial cell binding and spreading than a conventional planar material; in addition, the available sites for attachment are presentation in a highly restricted way. This geometry contrasts with previous studies in which cells either contact both nanotubes and an underlying substrate [2], or attach to high-density CNT compacts [3, 4].

3.2. *Cell morphology and proliferation*

The responses of MG63, A549, and FOB cell types were investigated at one- and seven-day time-points after seeding. It was found that cell attachment at one day was similar for all cell types on all surfaces (1612 ± 97 cells/cm^2 for MWCNTs, and 1701 ± 378 cells/cm^2 overall) (Suppl. figure – please see online version of paper). The majority of MG63 and A549 cells on the MWCNT surfaces were found to display reduced spreading in comparison to the control surfaces, whilst primary FOB cells showed reduced widening and, in some cases, increased elongation. Overall, the surface area covered by each cell was found to be dramatically reduced on the MWCNT surfaces (figure 2A).[†] During the seven-day period, the number of cells on the MWCNT substrates increased overall (figure 2B). Both the HOPG and glass control surfaces supported confluent cell layers after seven days in culture. In contrast, the MWCNT surfaces supported intermittent cell clusters (figure 3). Actin staining also revealed that cells attached to the nanotube surfaces extend prominent filopodia (figure 4).

3.3. *The actin cytoskeleton and focal adhesions*

To further investigate the effect of nanotubes on cell shape and formation of focal adhesions, cells placed in culture for 24 hr were immunostained for vinculin, an important focal adhesion linker protein. Different stages of focal adhesion formation are commonly identified in cells: dot-like structures initially form, which are thought to be the precursors to larger structures through recruitment of clusters of proteins and the binding of f-actin stress fibres [31]. After 24 hr in culture, all three cell types cultured on planar control surfaces developed significant FAs towards the cell edges, connecting the underlying substrate to f-actin stress fibres of the cytoskeleton (figure 5A, B, and C). In contrast, although dot-like FAs remain visible on the MWCNT samples, larger FA formations are restricted, possibly due to size constraints placed on FA enlargement by the nanotube diameter (figure 5D, E, and F).

[†] It should be noted that due to low seeding density necessary for study of individual cell areas, the absorbance values for the MTS assay on MWCNT substrates were also low: 0.08–0.17.

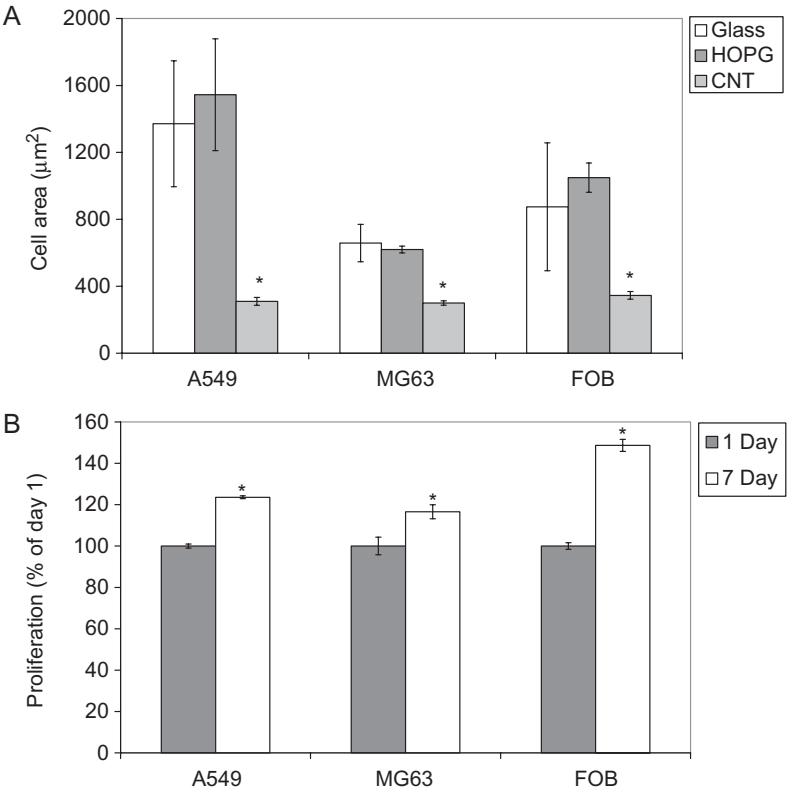

Figure 2. (A): Average cell spreading area after one day in culture on MWCNTs for each cell type. The asterisk indicates that cell spreading was significantly reduced ($p < 0.01$) for cells on MWCNTs for all cell types. (B): Cell proliferation on MWCNTs at seven days compared with one day for each cell type. The proliferation assay shows that cell number increased overall by seven days. The asterisk indicates a significant increase over seven days ($p < 0.01$) compared with day 1.

3.4. *SEM investigation*

Through SEM imaging, we investigated cellular interaction at the interface with the MWCNTs. Cells were found to fully attach and in some cases surround the nanotubes (figure 6). The density of the MWCNT network and the relative size of the nanotubes in relation to cell size is evident. It was found that the cells did not break through the mesh, and were not able to penetrate into the surface.

4. Discussion

The development of nanofibrous scaffolds for biological use has many advantages, including increased binding area for cell recognized ligands, increased nanoporosity, and faster transport of nutrients and signalling factors throughout the scaffolds [12, 16, 25]. However, the relationship between nanofibre size, fibre density and cell response remains undetermined. Towards this end, we investigated the response

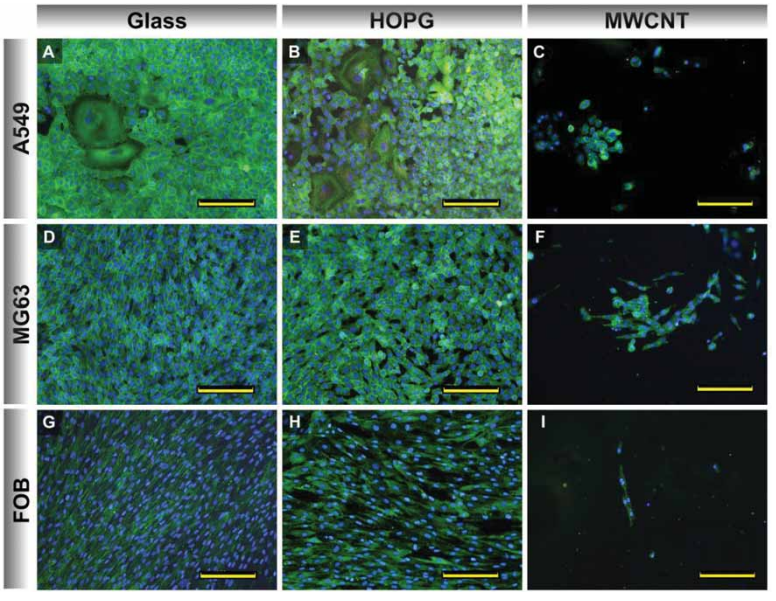

Figure 3. Fluorescent staining of the f-actin cytoskeleton (green) and DNA (blue), showing cell attachment after seven days in culture. All cell types were found to spread and proliferate on both glass and HOPG controls, and formed confluent cell layers after seven days (A, B, D, E, G, and H). Cells cultured on the MWCNT surfaces (C, F, I) were not found to be confluent and although initially seeded uniformly across the surface, all cell types were mainly proliferating in clusters when observed after seven days. Scale bars = 200 μm. This figure is available in colour online.

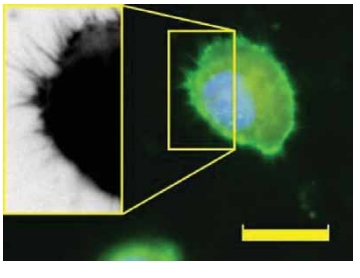

Figure 4. A representative MG63 cell found attached to the MWCNT surface after 24 hr, stained green for actin (phalloidin-FITC) and blue for DNA (DAPI) and imaged at 60× using fluorescent microscopy. Although many cells displayed a rounded morphology on the MWCNT surface, they were also found to extend prominent filopodia out into the surrounding area. Scale bar = 20 μm. This figure is available in colour online.

of two different cell lines and one primary cell type to culture on a network of 35 nm diameter MWCNTs, used as a model nanofibrous material.

In routine culture on flat surfaces, each cell type spreads to form different morphologies: A549s tend to spread equally in all directions, MG63s show widening and moderate elongation, and primary FOB cells tend to elongate more exaggeratedly than MG63 cells. In culture on MWCNTs, all cells tended to maintain their general

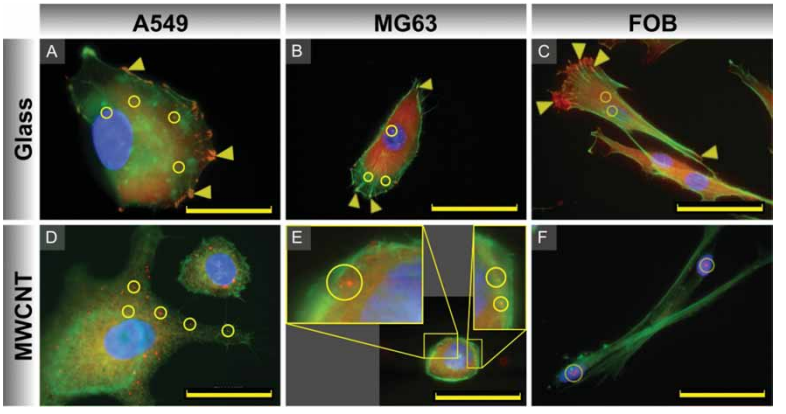

Figure 5. Fluorescent staining of f-actin (green), DNA (blue), and immunofluorescent staining of vinculin (red) after 24 hr in culture to reveal points of focal adhesion (indicated by arrows heads). Typically, cells cultured on flat surfaces spread and form larger focal contacts, as seen on glass (A, B, and C). Several different cell morphologies were seen on both glass and MWCNT surfaces. Cells attached to MWCNTs were more rounded (D upper right and E). Where cells were found to spread (D left and F), only smaller contacts were observed (indicated by circles). The spread FOB cells were found to show exaggerated elongation and reduced widening (F). Scale bars = 50 μm. This figure is available in colour online.

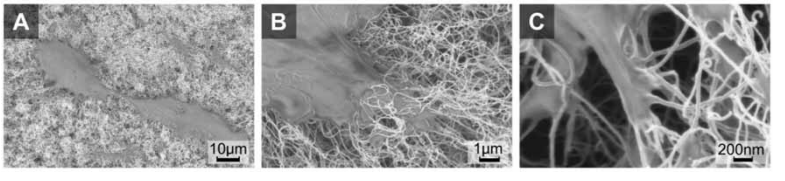

Figure 6. SEM imaging of MG63 interaction with MWCNTs after 24 hr in culture. MG63 cells attached and can be seen to spread across the CNT surface (A). Although the cells did not penetrate deeply beneath the top surface of the nanotube network, some interaction within the top layer can be seen (B). At high magnification, cell membrane protrusions appear to wrap around, and are possibly guided by the nanotubes (C).

morphological forms; however spreading and surface area covered was reduced (figure 2A). In some cases, FOB cells were found to elongate but not widen as they did on the flat controls (figure 5F). The cell proliferation assay revealed that cell number increased overall after seven days in culture (figure 2B). This result was seen for all cell types. At seven days, we observed that cells on the nanotube surface were clustered together (figure 3). The mechanisms behind these effects have not been determined; however, this response may result from increased local proliferation and reduced cellular migration. Other factors such as increased cell–cell contact may also be important.

For non-dense surfaces, the size and spacing of the features available for cell attachment will control the number of possible binding sites and usable area for cell spreading. For the MWCNT surfaces, SEM imaging revealed that the area available for initial cell attachment mainly consisted of separate non-bundled nanotubes, and

presented substantially less continuous surface area for cell spreading than an uninterrupted planar material (figure 1C). Imaging at high magnification revealed that cells interact with and spread along the nanotubes, although they did not penetrate into the network (figure 6). The interaction between nanotubes and individual filopodia was not explored because the fine cell structure was damaged by the dehydration procedure used in sample preparation. This interaction is evident through actin staining and fluorescent imaging, which reveals that long filopodia extend from MG63 cells onto the MWCNT surfaces (figure 4). It has been suggested that cells use filopodia to sense the surrounding nanoscale landscape [32], although the mechanisms behind this are not fully understood.

On the control surfaces, the flat topology allows larger FA formation, and strong tethering of the cytoskeleton to the base substrate. In turn, this allows full development of cytoskeletal stress fibres, resulting in further strengthening of the focal adhesions and further cell broadening. Chen *et al*. reported that FA formation not only resulted from opportunistic binding of the cell to adhesion proteins adsorbed onto the substrate, but also that the cell's global cytoskeletal shape plays an important role in directly influencing FA assembly and organization [29]. This results in strong anchoring of the cytoskeleton and helps in the process of elongation. It has been reported that well-established FAs stimulate increased cell-signalling activity [26] and that the size of FAs greatly influences subsequent cell behaviour: a reduction in FA size may have a direct effect on subsequent proliferation and the expression of ECM.

When taking into account the role of fibre diameter and density in influencing cellular response, other factors also must be considered. Cellular response to materials in culture is typically characterized by a cell's ability to proliferate and spread across a surface: effectively a wound healing response. Cells are seeded at low density and must proliferate to come into contact with other cells. In tissues, the opposite is true, and cell-to-cell contact is vital for tissue development and function [33, 34]. The three-dimensional (3D) nature of tissue is likely to play a significant role in governing cell behaviour [35, 36]. Whilst developing biomimetic materials with nanofibre dimensions and densities similar those found in the ECM, the final context must be kept in mind. In this study, the complex nature of the 3D nanofibrous ECM has been reduced to a fibrous, yet planar environment. This simplification enables the long-term cellular interaction with nanofibrous structures to be investigated more easily.

As well as considering the role that the structure and distribution of attachment area plays in influencing cellular response, it is interesting to explore how individual nanotubes affect protein attachment and conformation. It has been reported that, when sonicated, single strands of DNA will wrap around SWCNTs [37]. Protein binding and conformation to SWCNTs is also influenced by the conformational flexibility and hydrophobicity of the sequences of amino acids [38]. In this way, the nanotube dimensions can effect the binding and conformation of ECM proteins, in turn modifying integrin binding [39], which may lead to changes in deposition of ECM, cell migration and cell fate. Investigations in this area are ongoing and we look forward to further comparative studies on similar scale systems with different surface chemistries and orientations.

5. Conclusions

Nanofibrous materials offer many possible advantages to the tissue engineering and biomaterials research community [12, 16, 25]. In this study, we investigate the cellular response to a network of MWCNTs, as a model nanofibrous system. This model provides a fibrous, yet accessible planar environment that can be investigated through standard two-dimensional culture techniques. The nanotube surface is stiff with a well-defined but adjustable topology that cells are unable to penetrate or significantly alter. We found that cells were able to attach and proliferate over a seven-day period on the network of 35 nm nanotubes, even though they were not able to penetrate the network and were restricted to the surface area provided by the uppermost nanotubes. All three distinct cell types formed clusters on the MWCNT surfaces after seven days in culture. The cells in and around these clusters displayed a range of morphologies, but with reduced spreading. A number of FOB cells were also found to display reduced widening but increased elongation. For all cell types, proliferation was not comparable to planar control substrates, which supported confluent layers after seven days. Only smaller sized focal contacts were found on the nanotube substrates, and this may have affected cell migration and proliferation.

Acknowledgements

This work was made possible by funding from the EPSRC. We would also like to thank Ruth Pearce for her assistance with CNT fabrication.

References

[1] R. A. MacDonald, B. F. Laurenzi, G. Viswanathan, P. M. Ajayan, and J. P. Stegemann. Collagen–carbon nanotube composite materials as scaffolds in tissue engineering, J. Biomed. Mater. Res. A **74**, 489 (2005).
[2] V. Lovat, D. Pantarotto, L. Lagostena, B. Cacciari, M. Grandolfo, M. Righi, G. Spalluto, M. Prato, and L. Ballerini. Carbon nanotube substrates boost neuronal electrical signaling, Nano. Lett. **5**, 1107 (2005).
[3] J. L. McKenzie, M. C. Waid, R. Shi, and T. J. Webster. Decreased functions of astrocytes on carbon nanofiber materials, Biomaterials **25**, 1309 (2004).
[4] R. L. Price, K. Ellison, K. M. Haberstroh, and T. J. Webster. Nanometer surface roughness increases select osteoblast adhesion on carbon nanofiber compacts, J. Biomed. Mater. Res. A **70**, 129 (2004).
[5] B. Zhao, H. Hu, S. K. Mandal, and R. C. Haddon. A bone mimic based on the self-assembly of hydroxyapatite on chemically functionalized single-walled carbon nanotubes, Chem. Mater. **17**, 3235 (2005).
[6] S. K. Manna, S. Sarkar, J. Barr, K. Wise, E. V. Barrera, O. Jejelowo, A. C. Rice-Ficht, and G. T. Ramesh. Single-walled carbon nanotube induces oxidative stress and activates nuclear transcription factor-kappaB in human keratinocytes, Nano. Lett. **5**, 1676 (2005).
[7] A. A. Shvedova, V. Castranova, E. R. Kisin, D. Schwegler-Berry, A. R. Murray, V. Z. Gandelsman, A. Maynard, and P. Baron. Exposure to carbon nanotube material: assessment of nanotube cytotoxicity using human keratinocyte cells, J. Toxicol. Environ. Health A **66**, 1909 (2003).
[8] A. A. Shvedova, E. R. Kisin, R. Mercer, A. R. Murray, V. J. Johnson, A. I. Potapovich, Y. Y. Tyurina, O. Gorelik, S. Arepalli, D. Schwegler-Berry, A. F. Hubbs, J. Antonini, D. E. Evans, B. K. Ku, D. Ramsey, A. Maynard, V. E. Kagan, V. Castranova, and P. Baron. Unusual inflammatory and fibrogenic pulmonary responses to single-walled carbon nanotubes in mice, Am. J. Physiol Lung Cell Mol. Physiol **289**, L698 (2005).
[9] D. B. Warheit, B. R. Laurence, K. L. Reed, D. H. Roach, G. A. Reynolds, and T. R. Webb. Comparative pulmonary toxicity assessment of single-wall carbon nanotubes in rats, Toxicol. Sci. **77**, 117 (2004).

[10] N. A. Monteiro-Riviere, R. J. Nemanich, A. O. Inman, Y. Y. Wang, and J. E. Riviere. Multi-walled carbon nanotube interactions with human epidermal keratinocytes, Toxicol. Lett. **155**, 377 (2005).
[11] C. Singh, M. S. Shaffer, and A. H. Windle. Production of controlled architectures of aligned carbon nanotubes by an injection chemical vapour deposition method, Carbon **41**, 359 (2003).
[12] J. Venugopal and S. Ramakrishna. Applications of polymer nanofibers in biomedicine and biotechnology, Appl. Biochem. Biotechnol. **125**, 147 (2005).
[13] Z. Ma, M. Kotaki, R. Inai, and S. Ramakrishna. Potential of nanofiber matrix as tissue-engineering scaffolds, Tissue Eng. **11**, 101 (2005).
[14] D. S. Katti, K. W. Robinson, F. K. Ko, and C. T. Laurencin. Bioresorbable nanofiber-based systems for wound healing and drug delivery: optimization of fabrication parameters, J. Biomed. Mater. Res. **70B**, 286 (2004).
[15] M. M. Stevens and J. George. Exploring and engineering the cell-surface interface. *Science*, in press (2005).
[16] L. A. Smith and P. X. Ma. Nano-fibrous scaffolds for tissue engineering, Colloids Surf. B Biointerfaces. **39**, 125 (2004).
[17] H. Yoshimoto, Y. M. Shin, H. Terai, and J. P. Vacanti. A biodegradable nanofiber scaffold by electrospinning and its potential for bone tissue engineering, Biomaterials **24**, 2077 (2003).
[18] E. D. Boland, J. A. Matthews, K. J. Pawlowski, D. G. Simpson, G. E. Wnek, and G. L. Bowlin. Electrospinning collagen and elastin: preliminary vascular tissue engineering, Front. Biosci. **9**, 1422 (2004).
[19] F. Yang, R. Murugan, S. Wang, and S. Ramakrishna. Electrospinning of nano/micro scale poly(L-lactic acid) aligned fibers and their potential in neural tissue engineering, Biomaterials **26**, 2603 (2005).
[20] J. D. Hartgerink, E. Beniash, and S. I. Stupp. Self-assembly and mineralization of peptide-amphiphile nanofibers, Science **294**, 1684 (2001).
[21] N. B. Malkar, J. L. Lauer-Fields, D. Juska, and G. B. Fields. Characterization of peptide-amphiphiles possessing cellular activation sequences, Biomacromolecules. **4**, 518 (2003).
[22] S. Zhang. Fabrication of novel biomaterials through molecular self-assembly, Nat. Biotechnol. **21**, 1171 (2003).
[23] J. C. van Hest and D. A. Tirrell. Protein-based materials, toward a new level of structural control, Chem. Commun. (Camb.) **19**, 1897 (2001).
[24] M. P. Lutolf and J. A. Hubbell. Synthetic biomaterials as instructive extracellular microenvironments for morphogenesis in tissue engineering, Nat. Biotechnol. **23**, 47 (2005).
[25] K. M. Woo, V. J. Chen, and P. X. Ma. Nano-fibrous scaffolding architecture selectively enhances protein adsorption contributing to cell attachment, J. Biomed. Mater. Res. A **67**, 531 (2003).
[26] S. K. Sastry and K. Burridge. Focal adhesions: a nexus for intracellular signaling and cytoskeletal dynamics, Exp. Cell Res. **261**, 25 (2000).
[27] A. J. Garcia. Get a grip: integrins in cell-biomaterial interactions, Biomaterials **26**, 7525 (2005).
[28] A. Diener, B. Nebe, F. Luthen, P. Becker, U. Beck, H. G. Neumann, and J. Rychly. Control of focal adhesion dynamics by material surface characteristics, Biomaterials **26**, 383 (2005).
[29] C. S. Chen, J. L. Alonso, E. Ostuni, G. M. Whitesides, and D. E. Ingber. Cell shape provides global control of focal adhesion assembly, Biochem. Biophys. Res. Commun. **307**, 355 (2003).
[30] C. Salvador-Morales, E. Flahaut, E. Sim, J. Sloan, H. G. ML, and R. B. Sim. Complement activation and protein adsorption by carbon nanotubes, Mol. Immunol. **43**, 193 (2006).
[31] E. Zamir and B. Geiger. Molecular complexity and dynamics of cell-matrix adhesions, J. Cell Sci **114**, 3583 (2001).
[32] M. J. Dalby, M. O. Riehle, H. Johnstone, S. Affrossman, and A. S. Curtis. Investigating the limits of filopodial sensing: a brief report using SEM to image the interaction between 10 nm high nano-topography and fibroblast filopodia, Cell Biol. Int. **28**, 229 (2004).
[33] J. P. Thiery. Cell adhesion in development: a complex signaling network, Curr. Opin. Genet. Dev. **13**, 365 (2003).
[34] K. Vleminckx and R. Kemler. Cadherins and tissue formation: integrating adhesion and signaling, Bioessays **21**, 211 (1999).
[35] E. Cukierman, R. Pankov, D. R. Stevens, and K. M. Yamada. Taking cell-matrix adhesions to the third dimension, Science **294**, 1708 (2001).
[36] K. L. Schmeichel and M. J. Bissell. Modeling tissue-specific signaling and organ function in three dimensions, J. Cell Sci. **116**, 2377 (2003).
[37] M. Zheng, A. Jagota, E. D. Semke, B. A. Diner, R. S. McLean, S. R. Lustig, R. E. Richardson, and N. G. Tassi. DNA-assisted dispersion and separation of carbon nanotubes 2, Nat. Mater. **2b**, 338 (2003).
[38] Y. Lin, S. Taylor, H. Li, S. A. K. Fernando, K. Qu, W. Wang, L. Gu, B. Zhou, and Y. Sun. Advances toward bioapplications of carbon nanotubes, J. Mater. Chem. **14**, 527 (2004).
[39] B. G. Keselowsky, D. M. Collard, and A. J. Garcia. Integrin binding specificity regulates biomaterial surface chemistry effects on cell differentiation, Proc. Natl. Acad. Sci. USA **102**, 5953 (2005).